Supporting Information

Facile synthesis of Pt-decorated Ir black as bifunctional oxygen catalyst for oxygen reduction and evolution reactions

Dahui Fang[a,b], Xuejun Tang[a,b], Limeng Yang[a,b], Dongyan Xu[c], Hongjie Zhang[a], Shucheng Sun[a], Zhigang Shao[a,*] and Baolian Yi[a]

[a] *Fuel Cell System and Engineering Laboratory, Dalian Institute of Chemical Physics, Chinese Academy of Sciences,457 Zhongshan Road, Dalian 116023, China;*

[b] *University of Chinese Academy of Sciences, Beijing 100049, China;*

[c] *State Key Laboratory Base of Eco-chemical Engineering, College of Chemical Engineering, Qingdao University of Science and Technology, 99 Songling Road, Qingdao 266042, China;*

[*] *E-mail: zhgshao@dicp.ac.cn.*

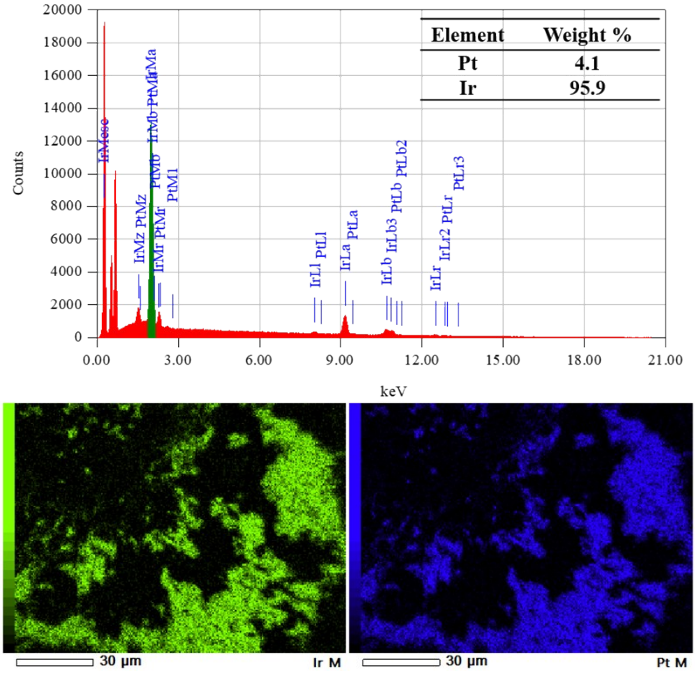

Fig. S1 SEM-EDX spectrum and corresponding element mappings for the iridium and platinum elements of $Pt_4@Ir_{96}$.

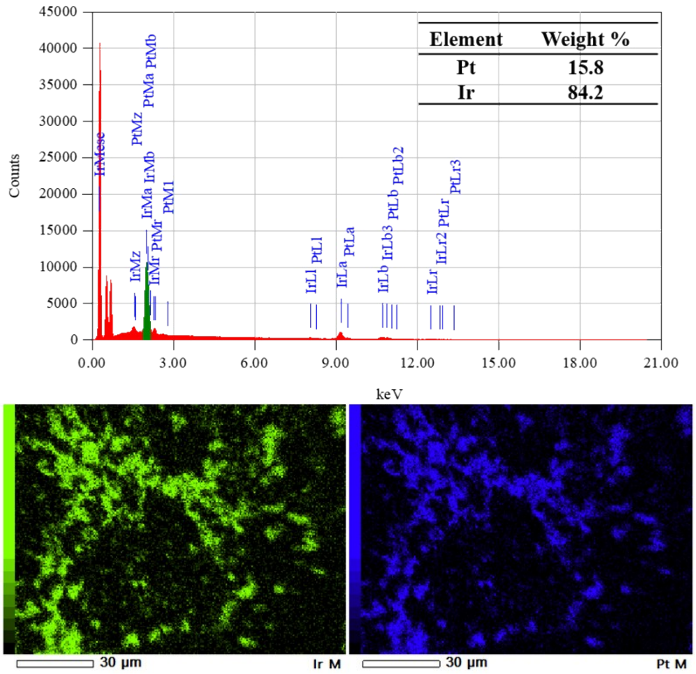

Fig. S2 SEM-EDX spectrum and corresponding element mappings for the iridium and platinum elements of $Pt_{16}@Ir_{84}$.

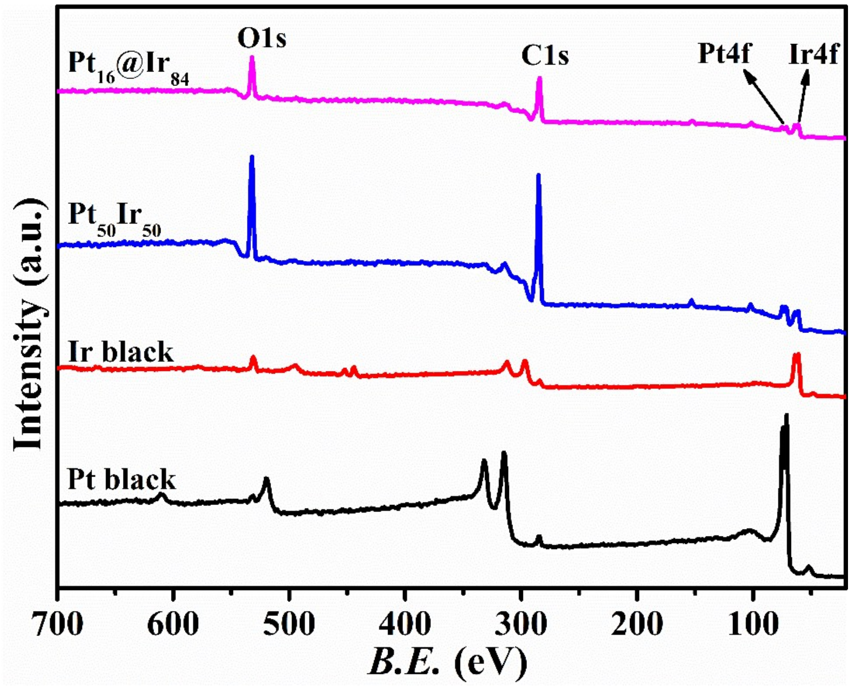

Fig. S3 XPS survey spectra of Pt black, Ir black, $Pt_{50}Ir_{50}$ and $Pt_{16}@Ir_{84}$.

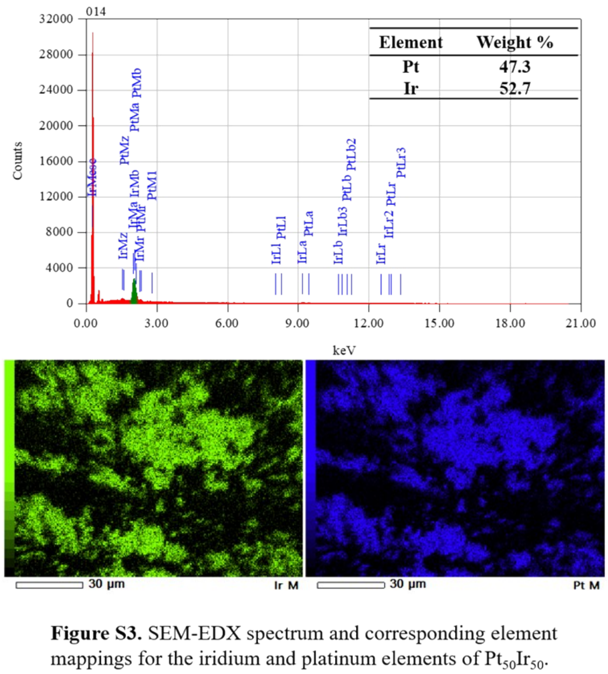

Fig. S4 SEM-EDX spectrum and corresponding element mappings for the iridium and platinum elements of $Pt_{50}Ir_{50}$.

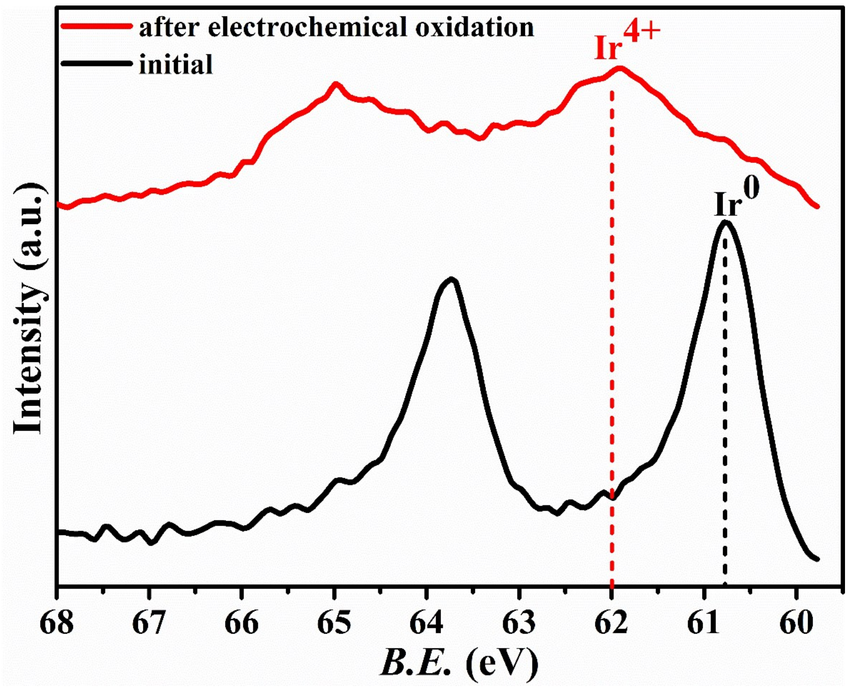

Fig. S5 Comparisons of high-resolution XPS spectra of Ir 4f for $Pt_{16}@Ir_{84}$ initial and after electrochemical oxidation process (0.05-1.42 V, 60 cycles, 100 mV s^{-1}).

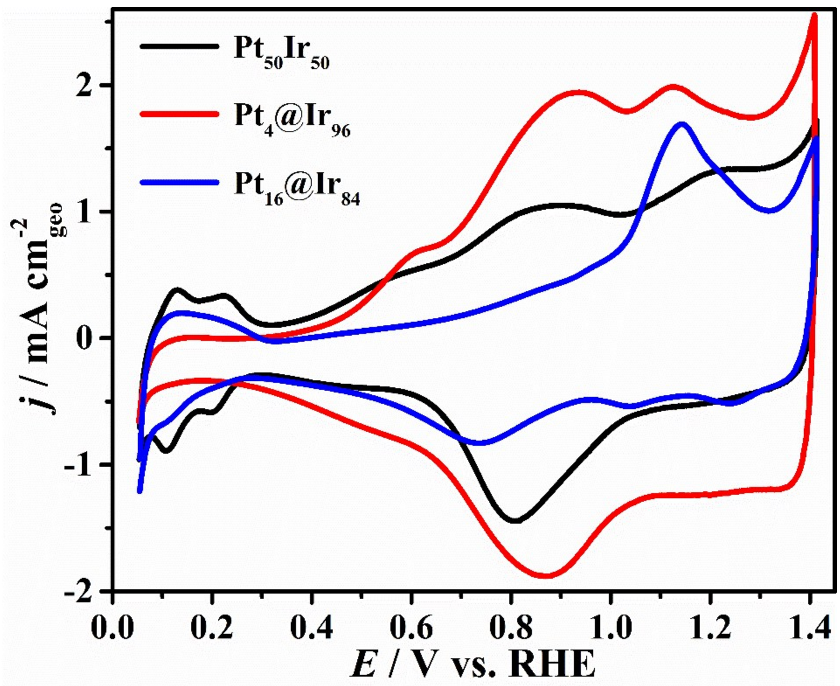

Fig. S6 CV curves recorded between 0.05 and 1.42 V after electrochemical oxidation process (0.05-1.42 V, 240 cycles, 100 mV s^{-1}) for $Pt_{50}Ir_{50}$, $Pt_4@Ir_{96}$ and $Pt_{16}@Ir_{84}$.

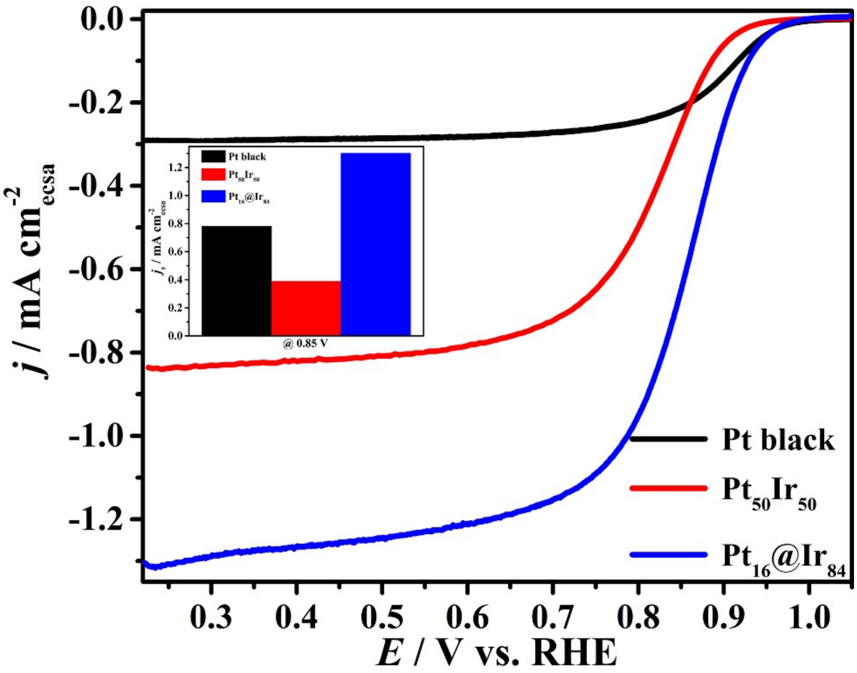

Fig. S7 ORR LSV curves for Pt black, $Pt_{50}Ir_{50}$ and $Pt_{16}@Ir_{84}$, with current normalized to the A_{ecsa} of Pt. The inset depicts their specific activities at 0.85 V calculated using Koutecky-Levich equation with background current subtracted and iR-drop corrected.

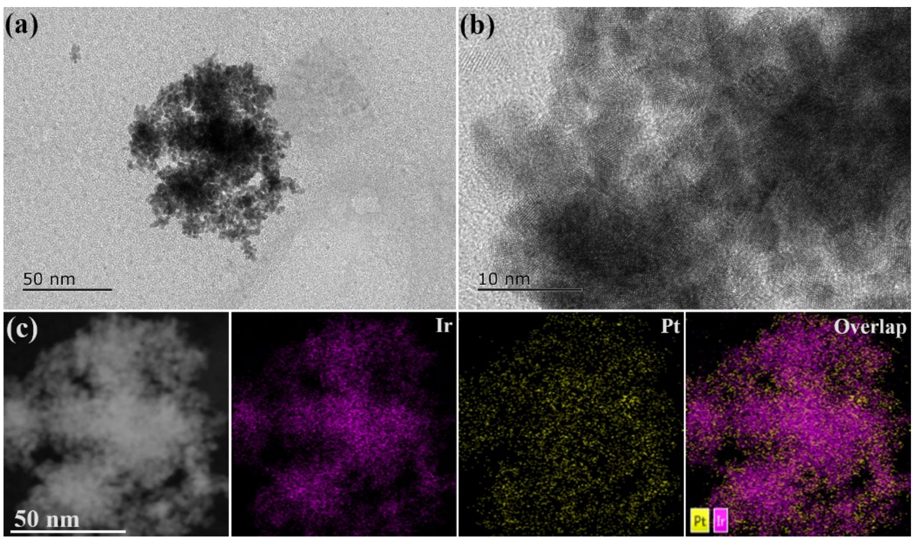

Fig. S8 TEM images (a) and (b), HAADF-STEM image and EDX mapping images (c) for Pt-decorated Ir black ($Pt_{16}@Ir_{84}$) after ORR test.

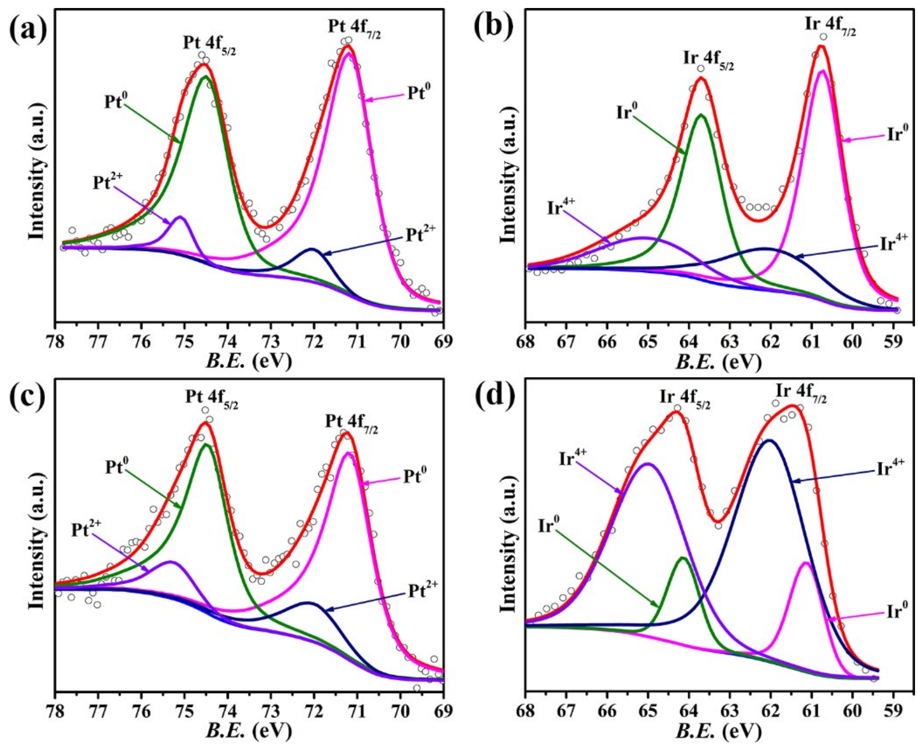

Fig. S9 High-resolution XPS spectra of (a) Pt 4f region and (b) Ir 4f region for Pt-decorated Ir black (Pt_{16}@Ir_{84}) after ORR test. High-resolution XPS spectra of (c) Pt 4f region and (d) Ir 4f region for Pt-decorated Ir black (Pt_{16}@Ir_{84}) after OER test.

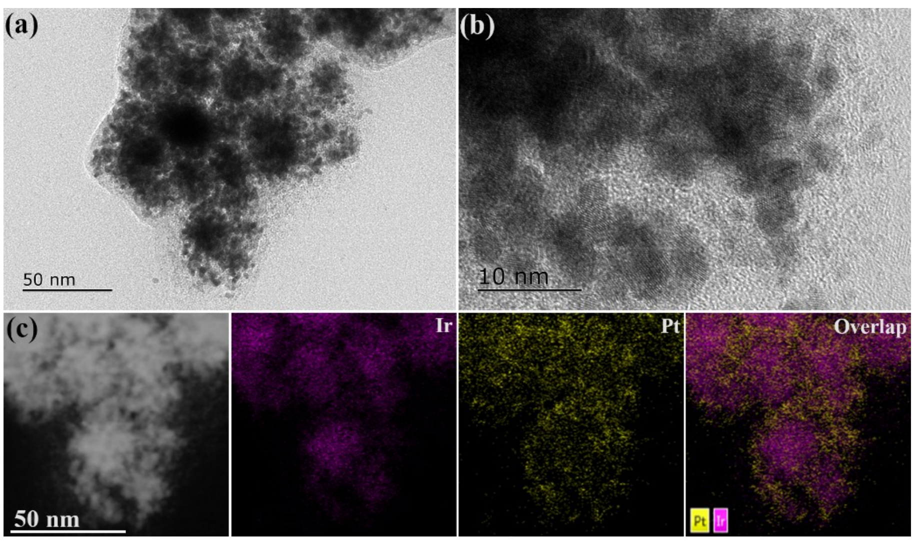

Fig. S10 TEM images (a) and (b), HAADF-STEM image and EDX mapping images (c) for Pt-decorated Ir black (Pt_{16}@Ir_{84}) after OER test.

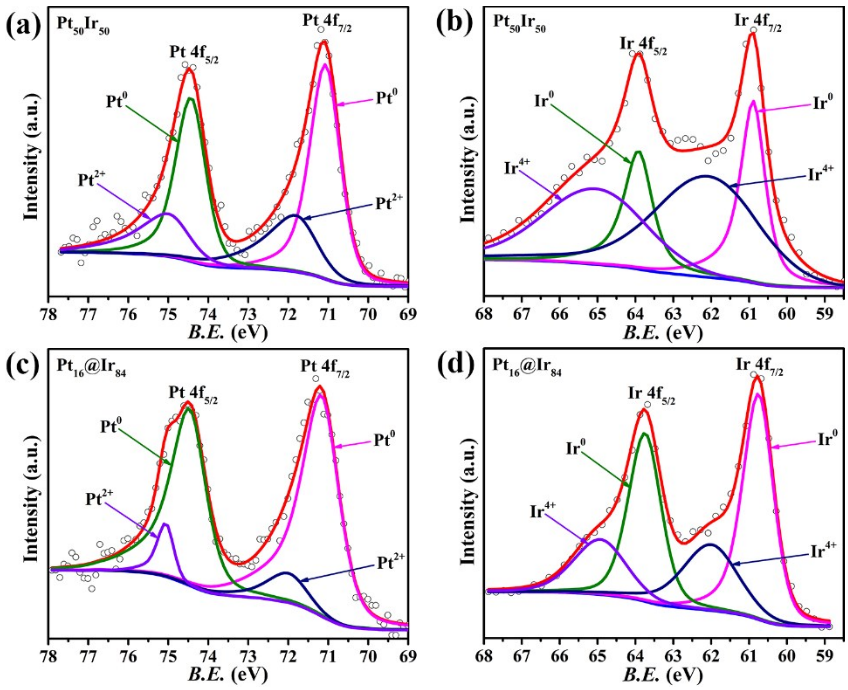

Fig. S11 High-resolution XPS spectra of (a) Pt 4f region and (b) Ir 4f region for $Pt_{50}Ir_{50}$ after ORR ADT test. High-resolution XPS spectra of (c) Pt 4f region and (d) Ir 4f region for Pt-decorated Ir black (Pt_{16}@Ir_{84}) after ORR ADT test.

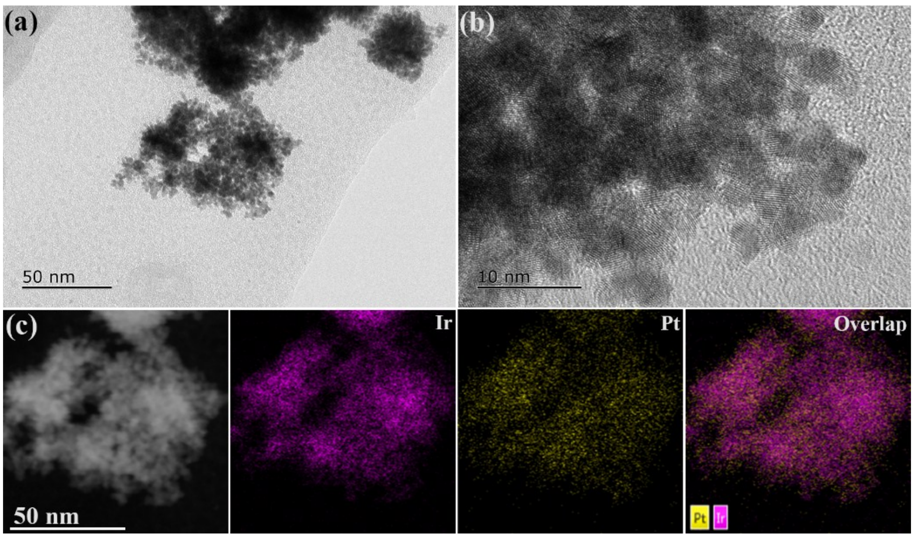

Fig. S12 TEM images (a) and (b), HAADF-STEM image and EDX mapping images (c) for Pt-decorated Ir black (Pt_{16}@Ir_{84}) after ORR ADT test.

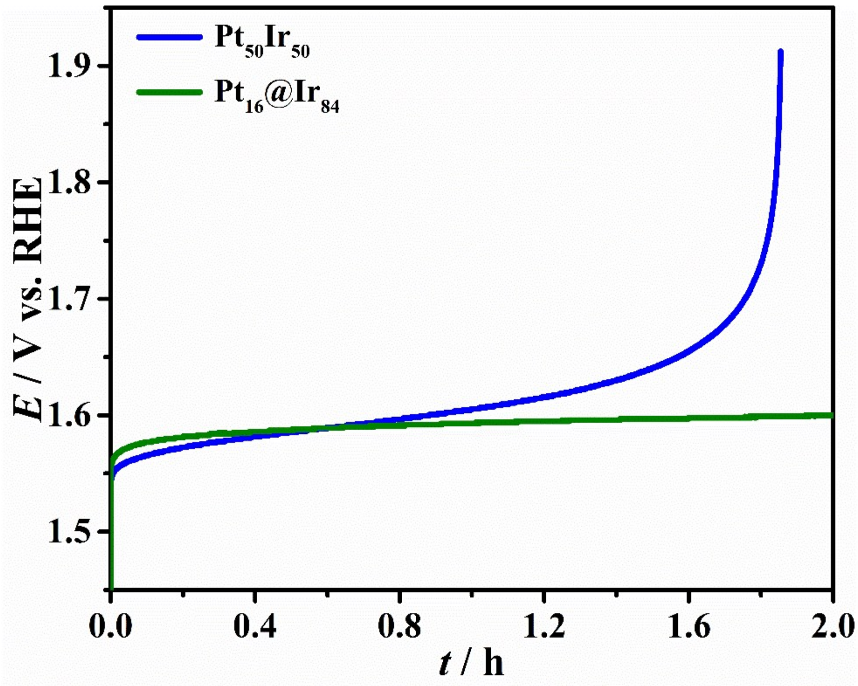

Fig. S13 Comparisons of chronopotentiometry curves for $Pt_{50}Ir_{50}$ and Pt-decorated Ir black ($Pt_{16}@Ir_{84}$) recorded at current density of 10 mA cm^{-2} in a N_2-saturated 0.1 mol L^{-1} $HClO_4$ solution.

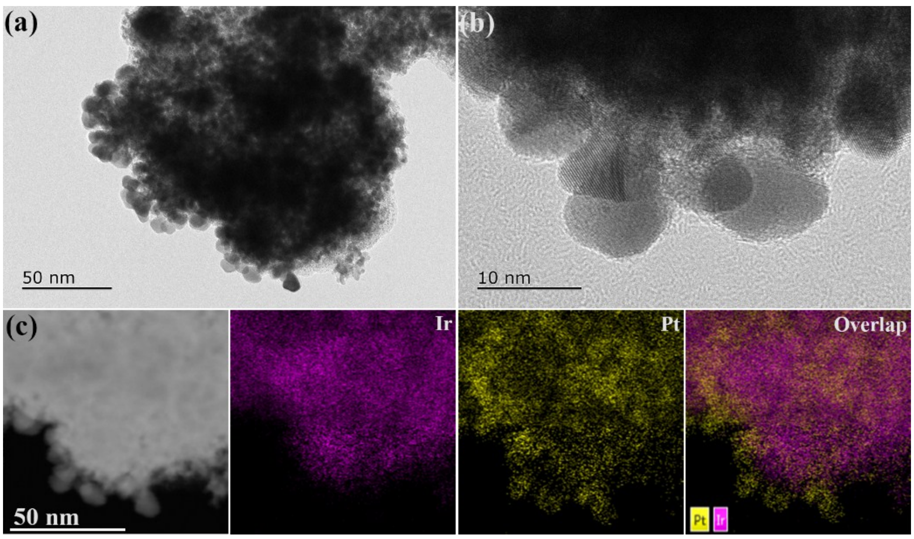

Fig. S14 TEM images (a) and (b), HAADF-STEM image and EDX mapping images (c) for Pt-decorated Ir black ($Pt_{16}@Ir_{84}$) after OER ADT test.

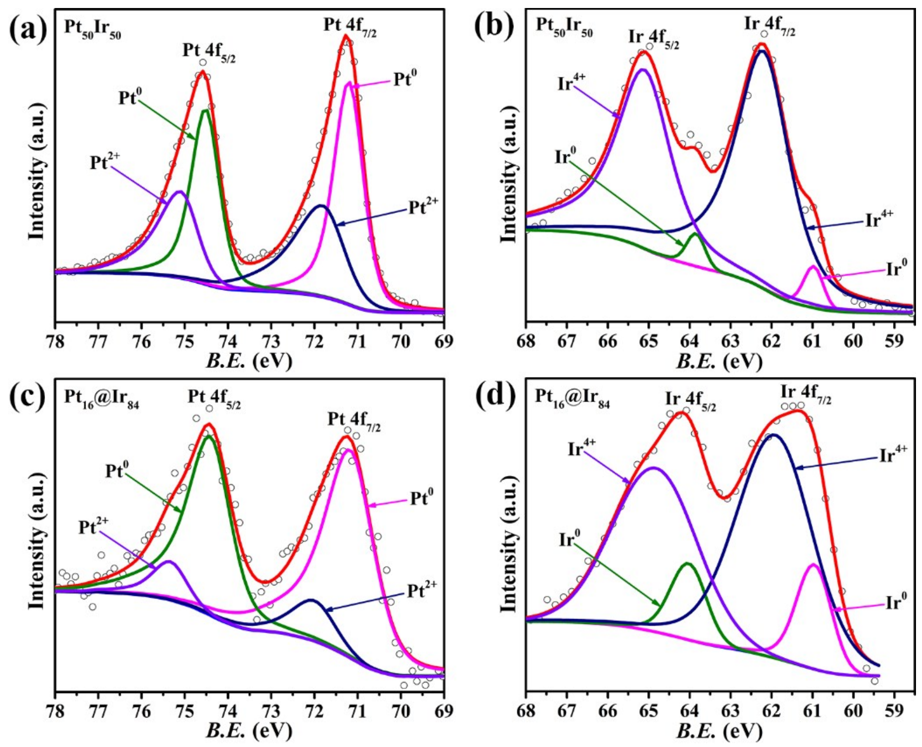

Fig. S15 High-resolution XPS spectra of (a) Pt 4f region and (b) Ir 4f region for $Pt_{50}Ir_{50}$ after OER ADT test. High-resolution XPS spectra of (c) Pt 4f region and (d) Ir 4f region for Pt-decorated Ir black ($Pt_{16}@Ir_{84}$) after OER ADT test.

Table S1 Surface atomic ratios, proportions of oxidation states taken from XPS analysis for $Pt_{16}@Ir_{84}$ catalyst initial and after ORR or OER test

Catalyst	Pt (%)	Ir (%)	Pt^0/Pt (%)	$Ir^0/Ir/$ (%)
initial	31.8	68.2	92.6	80.6
after ORR test	29.8	70.2	90.8	72.5
after OER test	20.8	79.2	83.6	17.6

Table S2 Comparisons of ORR mass activity at 0.85 V and OER mass activity at 1.53 V for $Pt_{50}Ir_{50}$ and $Pt_{16}@Ir_{84}$ catalysts evaluated initial and after ADT

Catalyst	j_k@0.85 V/mA mg_{Pt}^{-1}	j_m@1.53 V/mA mg_{Ir}^{-1}
$Pt_{50}Ir_{50}$ initial	53.8	214.8
$Pt_{50}Ir_{50}$ after ADT	15.6	91.0
$Pt_{16}@Ir_{84}$ initial	373.3	151.6
$Pt_{16}@Ir_{84}$ after ADT	314.6	175.6

Table S3 Comparisons of surface atomic ratios, proportions of oxidation states taken from XPS analysis for $Pt_{50}Ir_{50}$ and $Pt_{16}@Ir_{84}$ catalysts evaluated initial and after ORR ADT test

Catalyst	Pt (%)	Ir (%)	Pt^0/Pt (%)	$Ir^0/Ir/$ (%)
$Pt_{50}Ir_{50}$ initial	46.6	53.4	70.6	88.3
$Pt_{50}Ir_{50}$ after ADT	23.7	76.3	66.3	35.4
$Pt_{16}@Ir_{84}$ initial	31.8	68.2	92.6	80.6
$Pt_{16}@Ir_{84}$ after ADT	26.4	73.6	88.2	66.1

Table S4 ICP-OES results for $Pt_{50}Ir_{50}$ and $Pt_{16}@Ir_{84}$ catalysts tested after ORR ADT

Catalyst	Pt content in electrolyte /ppm	Pt mass retention ratio /%	Ir content in electrolyte /ppm	Ir mass retention ratio /%
$Pt_{50}Ir_{50}$	0.217	54.7	0.019	96.1
$Pt_{16}@Ir_{84}$	0.017	88.8	0.028	96.5

Table S5 Comparisons of surface atomic ratios, proportions of oxidation states taken from XPS analysis for $Pt_{50}Ir_{50}$ and $Pt_{16}@Ir_{84}$ catalysts evaluated initial and after OER ADT test

Catalyst	Pt (%)	Ir (%)	Pt^{2+}/Pt (%)	Ir^{4+}/Ir/ (%)
$Pt_{50}Ir_{50}$ initial	46.6	53.4	29.4	11.7
$Pt_{50}Ir_{50}$ after ADT	75.7	24.3	44.1	95.5
$Pt_{16}@Ir_{84}$ initial	31.8	68.2	7.4	19.4
$Pt_{16}@Ir_{84}$ after ADT	20.4	79.6	13.8	82.6

Table S6 ICP-OES results for $Pt_{50}Ir_{50}$ and $Pt_{16}@Ir_{84}$ catalysts tested after OER ADT

Catalyst	Pt content in electrolyte /ppm	Pt mass retention ratio /%	Ir content in electrolyte /ppm	Ir mass retention ratio /%
$Pt_{50}Ir_{50}$	0.112	76.6	0.300	37.4
$Pt_{16}@Ir_{84}$	0.029	81.0	0.065	91.9

Table S7 Comparisons of potential gap (ΔE) between the OER potential at a current density of 10 mA cm^{-2} ($E_{j=10}$) and the ORR potential at a current density of -3 mA cm^{-2} ($E_{j=-3}$) for $Pt_{50}Ir_{50}$ and $Pt_{16}@Ir_{84}$ catalysts evaluated after ADT

Catalyst	OER	ORR	ΔE
	Potential at 10 mA cm^{-2} ($E_{j=10}$/V)	Potential at -3 mA cm^{-2} ($E_{j=-3}$/V)	$= E_{j=10}-E_{j=-3}$ /mV
$Pt_{50}Ir_{50}$	1.592	0.761	831
$Pt_{16}@Ir_{84}$	1.519	0.838	681